ON THE RELATION BETWEEN LARGE-SCALE CORONAL WAVES AND METRIC TYPE II SOLAR RADIO BURSTS

A. Warmuth*, G. Mann*, and H. Aurass*

Abstract

Propagating shocks in the solar corona have been observed as type II radio bursts for over half a century. Another observational signature of large-amplitude perturbations are Moreton waves observed in Hα, and indeed several studies have suggested that Moreton waves and type II bursts are closely associated. During the last few years waves features were detected in additional wavelength bands such as EUV or soft X-rays, but whether these signatures are created by a common mechanism has remained controversial. We present new soft X-ray observations of globally propagating coronal waves obtained with the Solar X-ray Imager (SXI) aboard *GOES*-12. Due to their high temporal cadence, SXI data prove that all signatures of coronal waves are created by the same physical disturbance. The behavior of this disturbance is consistent with a large-amplitude simple MHD wave that is at least partly shocked. In addition we show that the metric type II bursts that were observed in our events are kinematically consistent with the wavefronts. This implies that both coronal waves and metric type II bursts are caused by the same coronal disturbance. Due to its high cadence and duty cycle SXI is an ideal instrument to study this relation.

1 Introduction

Shocks propagating through the solar corona are most conveniently observed via the radio radiation they generate, which takes the form of narrow-band emission drifting from higher to lower frequencies. These *type II radio bursts* [for a review, see e. g. Mann, 1995a] were first interpreted as the signature of a collisionless fast-mode MHD shock by Uchida [1960].

With regard to the origin of type II bursts, no consensus has yet been reached. Usually a flare-ignited blast wave scenario [e. g. Vršnak & Lulić., 2000] and a CME-driven shock [e. g. Cliver et al., 1999] are considered. Flare-generated disturbances usually cannot penetrate to IP space, which is probably due to a local maximum of the Alfvén

* *Astrophysikalisches Institut Potsdam, An der Sternwarte 16, D–14482 Potsdam, Germany*

speed in the higher corona [e. g. Warmuth & Mann, 2005]. Therefore, most decametric/hectometric/kilometric type II bursts are generated by CME-driven shocks [e. g. Reiner et al., 2001].

The situation is more complicated for the coronal shocks that generate *metric type II bursts*. There is evidence that both flares *and* CMEs can create such shocks [e. g. Classen & Aurass, 2002]. One of the main difficulties in identifying the sources of these disturbances is our limited knowledge of their kinematics. Radiospectral data of type II bursts yield only a speed along the density gradient. Moreover, this speed is dependent on the density gradient. On the other hand, radioheliographic data are available only for a few frequencies and with low spatial resolution. Given these limitations, the comparison of type II and CME propagation or the back-extrapolation of the type II propagation in order to find the time and location of the ignition of the shock might yield ambiguous results.

Another signature of large-amplitude disturbances in the solar corona are globally propagating *coronal waves*. They were originally observed in Hα as arc-shaped fronts propagating away from flaring/erupting active regions with speeds of the order of 1 000 km s^{-1} [e. g. Moreton, 1960]. Moreton waves were interpreted to be the ground track of a dome-shaped coronal fast-mode wavefront that sweeps over the chromosphere [Uchida, 1968]. The same wavefront could also generate type II bursts, provided that at least a part of the wave has steepened to a shock [Uchida, 1974]. Indeed, the comparison of timing and velocities in individual events suggested a close association between the two phenomena [e. g. Harvey et al., 1974].

Provided that metric type II bursts and coronal waves are generated by the same disturbance, the waves can be used to constrain the kinematics of this perturbation more tightly than it is possible from radiospectral observations alone. This is mainly because the measurement of their kinematics is not dependent on density and because accurate 2D spatial information is available. It is thus possible to determine the launch time as well as the starting point of the perturbation, which can then be compared to the evolution of the associated flare and CME in order to identify the cause of the disturbance.

A prerequisite for this approach is a better understanding of coronal waves and their relation to the radio bursts. The EIT instrument aboard *SOHO* ([Delaboudinière et al., 1995] has recorded a large number of globally propagating coronal waves [Thompson et al., 1998] in the EUV. However, whether these "EIT waves" are the coronal counterpart to Moreton waves is still being debated, since they are 2-3 times slower than Moreton waves, appear much more frequently and usually have a more diffuse and irregular morphology [e. g. Klassen et al. 2000]. Unfortunately, the low cadence of EIT does not allow a precise determination of the kinematics of the waves, whereas Hα data show the fronts only comparatively close to the source.

Like the EUV, soft X-ray (SXR) observations offer the opportunity to observe the coronal waves directly, not just their chromospheric signatures. A few waves were observed with *Yohkoh*/SXT, and it was shown that they match the kinematical curves of the associated Moreton waves [e. g. Khan & Aurass 2002]. Due to the small FOV in SXT's flaring mode, these waves could not be traced far enough in order study their relation with global EIT

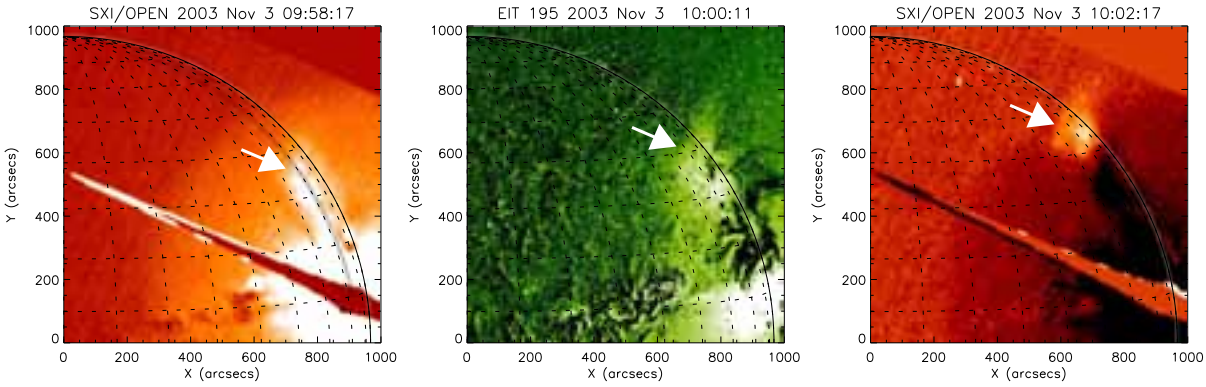

Figure 1: The propagation of the coronal wave of 2003 November 3 as shown by SXI (left, right) and EIT 195 Å (middle) running difference images. The wave is indicated by arrows. Note that the morphology of the wavefront is similar in SXR and EUV.

.

waves. This is now possible with the Solar X-ray Imager (SXI) aboard the GOES-12 satellite [Hill et al., 2005]. It provides full-disk coverage and a superior time cadence as compared to EIT, and we have succeeded in detecting coronal waves with SXI.

In this communication, we employ these "SXI waves" – using six events from October and November 2003 – to constrain the physical nature of large-scale coronal waves. In addition, we compare the characteristics of coronal waves to those of the associated metric type II bursts, and show that they are indeed created by a common disturbance.

2 Observations with GOES/SXI

SXI is a grazing-incidence telescope which provides full-disk solar images (with a resolution of 5" per pixel) using various analysis filters. For observing coronal structures, long-exposure (3 sec) images in the temperature range of 3–5 MK are used. Between 2003 October 29 and 2003 November 4, such images were available at a cadence of 2–4 min. In this period the active regions (ARs) 10486 and 10488 produced numerous energetic flares and CMEs. We found six wave events in the SXI data (labelled E1 to E6 in this work), all of which were also observed by EIT. With the exception of one event, all were associated with strong flares, as well as with CMEs and metric type II bursts.

Figure 1 shows two running difference images of the best-defined SXI wave event associated with an X3.9 flare and a fast CME on 2003 November 3. The wavefront is clearly visible as an area of increased emission propagating away from AR 10488. The front extends also above the solar limb to heights of ≈ 100 Mm. The EIT difference image also included in Fig. 1 shows that EUV and SXR signatures are very similar. The broadly comparable brightness increase over the range from 1.5 to 4 MK implies that the coronal disturbance must be compressive and cannot solely be due to temperature changes.

In order to determine the relation of the SXI waves to the chromospheric signatures, we have checked the events for wave signatures in Hα and He I (using data from the solar

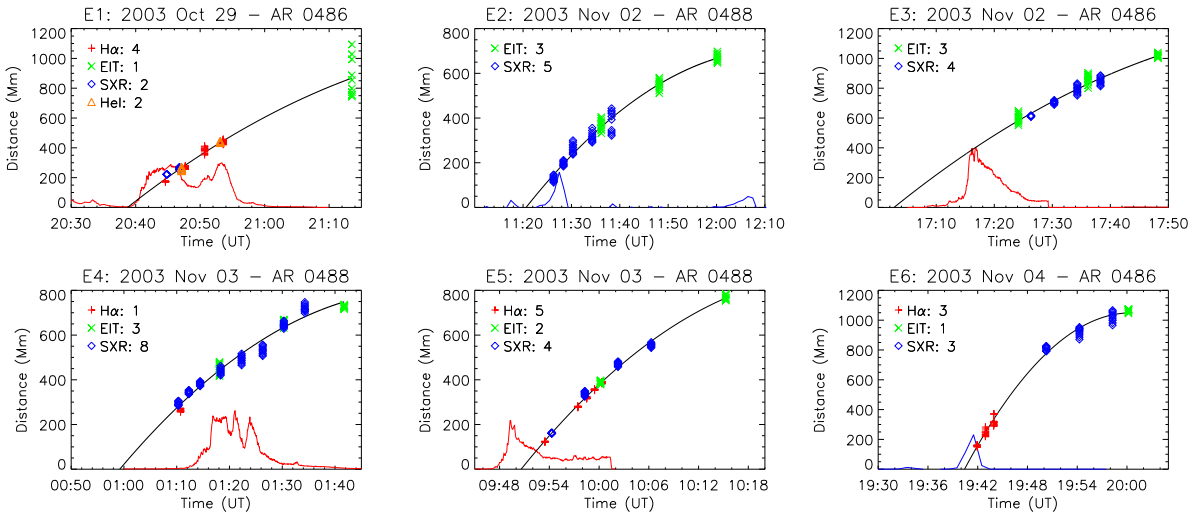

Figure 2: Kinematics of the coronal wave events [after Warmuth et al., 2005]. The distances of the leading edges are plotted together with 2nd degree polynomial fits. Distances are given in Mm (10^3 km). Also included are HXR lightcurves of the associated flares.

observatories Kanzelhöhe, Big Bear and Mauna Loa). Hα waves were found in four events, while weak He I signatures were present in one case. The distances of the leading edges from the center of the flare were measured along ten great circles [cf. Warmuth et al., 2004a] for all SXI, EIT, Hα and He I wavefronts. The result is shown in Fig. 2, where also the numbers of fronts in the various spectral bands are given. Hard X-ray (HXR) lightcurves (25 - 50 keV; plotted in arbitrary units) from *RHESSI* [Lin et al., 2002] are included at the bottom of each graph to show the context of the associated flares (for the events E2 and E6, the derivative of the flux in the 3 - 25 keV GOES channel is shown as a proxy for the HXR emission). The majority of the waves are apparently launched near the impulsive energy release phase, while E3 and E4 seem to start up to 10 min earlier.

Figure 2 shows that the wavefronts are consistent with a single physical disturbance causing the different signatures. This confirms the findings of Warmuth et al. [2004a]. Deceleration is present in all events, and the kinematical parameters derived closely correspond to the results of Warmuth et al. [2004a], which means that we are studying the same class of events. It is also evident from Fig. 2 that SXI wavefronts can be observed close to as well as far away from the starting location. They thus represent a missing link between Moreton and EIT waves. This is also reflected by the fact that their deceleration and mean speeds lie in between the values found for Moreton and EIT waves [Warmuth et al., 2005]. Thus SXI observations sample *both* propagation regimes: the vicinity of the AR where the wave is fast and strongly decelerating, and the more remote areas of the quiet corona where the disturbance has a lower and nearly constant speed.

The ubiquitous deceleration, combined with the decrease of the waves' intensities and the increase of their thickness, is typical for a shock formed from a large-amplitude magneto-hydrodynamic simple wave [cf. Mann, 1995b]. Since the trailing edge has a small amplitude, it moves with the fast magnetosonic speed v_{ms}, whereas the leading edge propagates

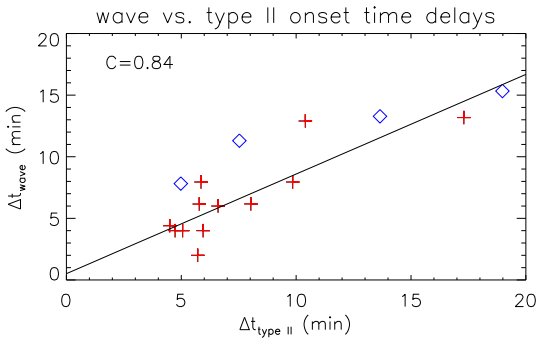

Figure 3: Correlation between the onset time delays (with respect to the SXR flare onset) of type II burst (Δt_{typeII}) and Moreton waves (Δt_{wave}). A linear fit of the data points is shown, and the correlation coefficient C is indicated. Additional data points (diamonds) show the correlation between Δt_{typeII} and the onset time delay of four SXI waves.

supermagnetosonically at $v_{lead} = M_{ms} v_{ms}$, where $M_{ms} > 1$ is the magnetosonic Mach number. This causes a broadening of the perturbation profile, and combined with the geometric expansion, this leads to a drop in the perturbation amplitude, which also means that the disturbance will slow down and may finally decay to a linear wave propagating at v_{ms}. We stress that the observed waves all decelerated to comparable speeds, as given for example by the mean EIT speed $\langle \bar{v}_{EIT} \rangle = 320 \pm 120$ km s^{-1}. This agrees very closely with the value of $\langle \bar{v}_{EIT} \rangle = 311 \pm 84$ km s^{-1} found by Warmuth et al. [2004a]. These velocities thus do not reflect properties connected to an individual event, but rather the characteristic speed of the ambient medium, i.e. v_{ms}. This supports the notion that in the regions far from the source AR the disturbances are fast-mode waves.

3 Relation of waves and type II bursts

After having established that indeed all wavefronts are created by a single disturbance, we can now study how this perturbation relates to the associated metric type II bursts. Recently Warmuth et al. [2004b] have shown that probably *all* Moreton waves are accompanied by metric type II bursts. Moreover, close correlations between Moreton and type II kinematics and timing were found, which strongly suggests that Moreton waves and type II bursts are signatures of the same disturbance. This is supported by observations with the Nançay radioheliograph, which have shown for two events that the type II burst sources are closely associated with the Moreton wavefronts [Gopalswamy et al., 2000; Khan & Aurass, 2002].

As an example, the crosses in Fig. 3 show the correlation between the Moreton wave and type II burst onset time delays Δt (i.e, the time lags between wave/burst onset and the start of the associated SXR flare) for the 12 events of Warmuth et al. [2004b]. The later the Moreton wave is observed, the later the burst will start, too, which implies that the expansion of the disturbance (i.e. the shock geometry) is broadly self-similar in the different events.

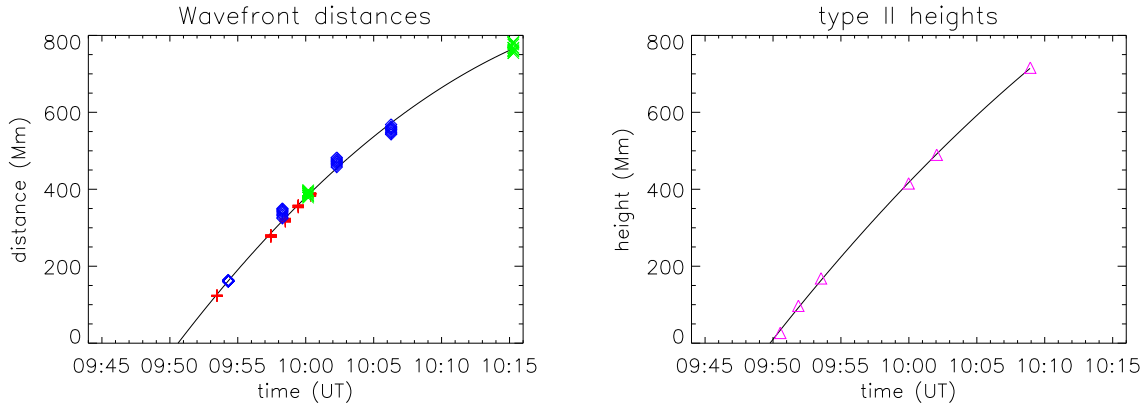

Figure 4: Left: Kinematics of the coronal wave of 2003 Nov 03. Symbols are as in Fig. 2. Right: Kinematics of the metric type II burst associated with the same event. The heights were calculated using a one-fold Newkirk density model. Note that the two kinematical curves agree closely during the first half of the propagation of the disturbance.

One problem with establishing these correlations is the scarcity of well-defined Moreton waves. SXI waves, which are more readily detectable, might be able to improve the situation, since they provide more information on the waves' kinematics than EIT. As a proof of this concept we have included in Fig. 3 the correlations between Δt_{typeII} and the onset time delay of four of our SXI waves (*diamonds*). It is evident that they show the same correlation as Moreton waves do.

Apart from these correlations, we also find that the kinematics of waves and type II bursts – bearing in mind the limitations mentioned in Sect. 1 – are very similar in the individual cases. To illustrate this, Fig. 4 shows the kinematical curves of the coronal wave of 2003 November 3 (using SXI, EIT and Hα fronts) and the associated type II burst (using a one-fold Newkirk density model) which was observed by the Potsdam-Tremsdorf radio spectral polarimeter [Mann et al., 1992]. Both phenomena are launched at the same time and have similar initial speeds. However, the wavefronts decelerate more strongly than the burst source, presumably because it is propgating through a denser medium.

4 Conclusion

We conclude that a coronal transient that is observable with EIT will generally also be imaged by SXI. The SXI observations presented here are consistent with the scenario of a large-amplitude simple wave which is at least partly shocked and which generates all signatures in the various spectral ranges. Furthermore, we have presented strong evidence for the notion that this perturbation generates both coronal waves and metric type II bursts. Note that the coronal waves we have studied are probably the high-amplitude limit of the phenomenon. There are many coronal waves without type II bursts, and they may be generated by a different mechanism.

SXI is ideally suited for a consistent study of how initially supermagnetosonic coronal

perturbations decay to ordinary fast-mode waves. The high cadence of SXI also allows for a better kinematical characterization of the waves even when supplementary data such as Hα images are not available or when the event is too weak to produce chromospheric signatures. Given the high duty cycle of SXI, this means that over the next few years an event sample of hundreds of kinematically resolved coronal waves will be compiled. This large data set will hopefully allow us to solve some of the long-standing issues regarding coronal waves and shocks, the most important one being the question of how these disturbances are launched.

Acknowledgements

The work of A. W. was supported by the German Space Agency DLR under grant No. 50 QL 0001. We thank the NOAA Space Environment center for free access to SXI data which were obtained from the National Geophysical Data Center. Hα data were provided by the upgraded Patrol Telescope at Kanzelhöhe Solar Observatory, which is a joint project of Kanzelhöhe and the Astrophysikalisches Institut Potsdam. The authors are grateful to the *RHESSI* Team (PI: R. P. Lin) for the free access to the *RHESSI* data and the development of the software. *SOHO* is a project of international cooperation between ESA and NASA.

References

Classen, H. T., and H. Aurass, On the association between type II radio bursts and CMEs, *Astron. Astrophys.*, **384**, 1098–1106, 2002.

Cliver, E. W., D. F. Webb, and R. A. Howard, On the origin of solar metric type II bursts, *Solar Phys.*, **187**, 89–114, 1999.

Delaboudinière, J.-P., and 27 co-authors, EIT: Extreme-Ultraviolet Imaging Telescope for the SOHO Mission, *Solar Phys.*, **162**, 291–312, 1995.

Gopalswamy, N., M. L. Kaiser, J. Sato, and M. Pick, Shock Wave and EUV Transient During a Flare, in *High Energy Solar Physics: Anticipating HESSI*, 2000STIN...0032759G, 32759, 2000.

Harvey, K. L., S. F. Martin, and A. C. Riddle, Correlation of a flare wave and type II burst, *Solar Phys.*, **36**, 151–155, 1974.

Hill, S. M., and 35 co-authors, The NOAA GOES-12 Solar X-Ray Imager (SXI) 1. Instrument, Operations, and Data, *Solar Phys.*, **226**, 255–281, 2005.

Khan, J. I., and H. Aurass, X-ray observations of a large-scale solar coronal shock wave, *Astron. Astrophys.*, **383**, 1018–1031, 2002.

Klassen, A., H. Aurass, G. Mann and B. J. Thompson, Catalogue of the 1997 SOHO-EIT coronal transient waves and associated type II radio burst spectra, *Astron. Astrophys. Suppl.*, **141**, 357–369, 2000.

Lin, R. P., and 65 co-authors, The Reuven Ramaty High-Energy Solar Spectroscopic Imager (RHESSI), *Solar Phys.*, **210**, 3–32, 2002.

Mann, G., H. Aurass, W. Voigt, and J. Paschke, *ESA-Journal*, **SP-348**, 129, 1992.

Mann, G., Theory and observations of coronal shock waves, in *Coronal Magnetic Energy Release,* edited by A. O. Benz and A. Krüger, Springer, Berlin, 183, 1995a.

Mann, G., Simple magnetohydrodynamic waves, *J. Plasma Phys.*, **53**, 109–125, 1995b.

Moreton, G. E., Hα Observations of Flare-Initiated Disturbances with Velocities $\sim$1000 km/sec, *Astron. J.*, **65**, 494–495, 1960.

Reiner, M. J., M. L. Kaiser, N. Gopalswamy, H. Aurass, G. Mann, A. Vourlidas, and M. Maksimovic, Statistical analysis of coronal shock dynamics implied by radio and white-light observations, *J. Geophys. Res.*, **106**, 25 279–25 290, 2001.

Thompson, B. J., S. P. Plunkett, J. B. Gurman, J. S. Newmark, O. C. St. Cyr, and D. J. Michels, SOHO/EIT observations of an Earth-directed coronal mass ejection on May 12, 1997, *Geophys. Res. Lett.*, **25**, 2465–2468, 1998.

Uchida, Y., On the Exciters of Type II and Type III Solar Radio Bursts, *Publ. Astron. Soc. Jap.*, **12**, 376–397, 1960.

Uchida, Y., Propagation of Hydromagnetic Disturbances in the Solar Corona and Moreton's Wave Phenomenon, *Solar Phys.*, **4**, 30–40, 1968.

Uchida, Y., Behavior of the flare produced coronal MHD wavefront and the occurrence of type II radio bursts, *Solar Phys.*, **39**, 431–449, 1974.

Vršnak, B., and S. Lulić., Formation of coronal MHD shock waves. II. The Pressure Pulse Mechanism, *Solar Phys.*, **196**, 181–197, 2000.

Warmuth, A., B. Vršnak, J. Magdalenić, A. Hanslmeier, and W. Otruba, A multiwavelength study of solar flare waves. I. Observations and basic properties, *Astron. Astrophys.*, **418**, 1101–1115, 2004a.

Warmuth, A., B. Vršnak, J. Magdalenić, A. Hanslmeier, and W. Otruba, A multiwavelength study of solar flare waves. II. Perturbation characteristics and physical interpretation, *Astron. Astrophys.*, **418**, 1117–1129, 2004b.

Warmuth, A., and G. Mann, A model of the Alfvén speed in the solar corona, *Astron. Astrophys.*, **435**, 1123–1135, 2005.

Warmuth, A., G. Mann, and H. Aurass, First soft X-ray observations of global coronal waves with the GOES Solar X-ray Imager, *Astrophys. J. (Letters)*, **626**, L121–L124, 2005.